MULTI-RIBBON PROFILE MONITOR USING CARBON GRAPHITE FOIL FOR J-PARC

Y. Hashimoto#, S. Muto, T. Toyama, D. Arakawa, Y. Hori, Y. Saito, M. Shirakata, M. Uota, Y. Yamanoi, KEK/J-PARC, Tsukuba/Tokai, Japan
S. Ohya, UBE Industries, Ltd., Organic Specialty Materials Research Laboratory, Ichihara, Japan
D. Ohsawa, Kyoto University, Radioisotope Research Center, Kyoto, Japan
M. Mitani, Minotos Engineering, Kunitachi, Japan
Y. Sato†, National Institute of Radiological Sciences, Chiba, Japan
T. Morimoto, Morimoto Engineering, Iruma, Japan

Abstract

We developed a secondary-electron-emission type beam profile monitor with a thin graphite ribbon target having a thickness of 1.6–2.0 μm. It clearly measured high-intensity beams up to 1×10^{13} ppb at a beam energy of 3 GeV with good linearity of the electron-emission yield. The energy deposition in this intense case was fairly small, 5.1×10^{-3} J/bunch/foil. The monitors were installed at injection beam transport (3-50 BT) for main ring (MR) primarily to measure the injection beam profiles by a single pass. A standard-size target has 32-channel ribbons 1.5–3 mm wide, with a length of 200 mm or more. The charge signal produced on the target was transmitted via a 34-channel coaxial cable assembly 400 m long to a signal processor without amplification. This paper describes the characteristics of the graphite, the target fabrication, and the results of beam measurements.

INTRODUCTION

In designing for secondary-electron-emission target, besides its material, target shape means wire or ribbon is worthy of consideration. Thin wires are typically employed [1, 2] because of they cause little beam loss. When handling high-intensity beams of more than 1×10^{13} particles per bunch (ppb) in GeV-class accelerators, the profile of not only the beam's core but also its tail becomes more important because of beam loss concerns. For high sensitive detection, a ribbon-type target [3, 4] is more suitable than a wire type's.

Although a ribbon's larger surface, as compared to that of a wire, can be advantageous for highly sensitive measurement, beam loss increases in proportion to the ribbon's width. To reduce beam loss, a material of lower atomic number is preferable, and target thickness should be decreased. Generally, the higher the melting point of a material, the more durable it is against heat load. Resistance to heat fatigue is desirable. On the other hand, the space charge effect on emitted dense electrons becomes significantly greater than it is for of an ordinary wire target, because the ribbon and electrode for electron capture are constructed in parallel. To overcome this effect, the potential applied to the electrode should be increased. In a high-intensity accelerator such as J-PARC, the target area becomes as large as 200 × 200 mm^2 or greater because of the larger beam size. More importantly, uniform electron emission is required over such a large area. In light of all these requirements, a specially developed graphite was chosen as the target material because of its low atomic number (6), high heat endurance, and small minimum thickness (1.6 μm).

#yoshinori.hashimoto@kek.jp
†deceased

THIN GRAPHITE TARGET

Figure 1: Graphite having thickness of 1.6 μm.

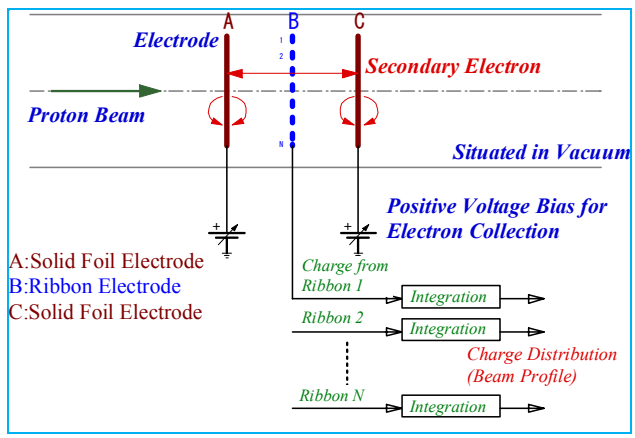

Figure 2: Detector configuration.

Graphite

The graphite was specially made by UBE Industries, Ltd. It has remarkable characteristics of flexibility and self-support, as shown in Fig. 1. These features are attributed primarily to its toughness, which results from the larger crystallites in its composition. Its firing temperature was 2600 °C, and the maximum size

manufactured was 160 × 320 mm^2 with a thickness of 1.6–2 μm.

Detector Configuration

The detector consisted of three electrodes as a unit (Fig. 2). Both outside electrodes were solid foils with positive potential, used for electron collection, and the middle electrode consisted of multiple ribbons; the charge signals produced on the ribbons were integrated in a circuit. Actually, to achieve both horizontal and vertical detection in one detector, the detector had only three solid-foil electrodes with a multi-ribbon electrode between each pair of foil electrodes; one ribbon electrode was for horizontal detection, and the other was for vertical detection.

Beam Energy Loss

Parameters related to energy loss and energy deposition for beam energy of 3 GeV are summarized in Tables 1 and 2, respectively. The beam is usually operated with eight bunches in the 3-50 BT every 3.52 s. A sufficiently small beam energy deposition of 4.1 × 10^{-2} J/cycle is estimated for a designed bunch intensity of 4 × 10^{13} ppb. Although temperature rise at the target depends on the beam density, estimated value by the engineering analysis system ANSYS© was less than 200 °C.

Table 1: Beam Energy Loss with 3-GeV Proton Beam

Parameter	Value
Atomic Number (z)	6
Material Energy Loss	2.0 [MeV·cm^2/g/proton]
Target Thickness	2 [μ m]
Total Energy Loss	0.8 [keV/proton]

Table 2: Energy Deposition by 3-50 BT Beam

Parameter	Value
Design Beam Intensity	4 × 10^{13} [ppb]
Energy Deposition by bunch/foil	5.1 × 10^{-3} [J/bunch]
Energy Deposition by 8 bunch/foil	4.1 × 10^{-2} [J/cycle]
Estimated Temperature Increase	Several 10s–200 [deg.]

Endurance Tests

To investigate the robustness of the foil against beam impact, two types of beam tests were conducted. The beam parameters are summarized in Table 3.

Table 3: Beam Parameters for Endurance Tests

Parameter	Long-Run Test	High-Temp. Test
Beam Species	Proton	Ne^+
Beam Energy	500 [MeV]	3.2 [MeV]
Beam Intensity	2 × 10^{12} [ppb]	3.0 [micro amp]
Repetition	20 [Hz]	Continuous
Beam Size	45^H × 15^V [mm^2]	8 [mm, dia.]

The first was a long-run test in which beams hit the target foil during a net 11 months of running. The total proton hit number amounted to more than 5 × 10^{20}, but the foil survived (Fig. 3[a]). The second was a high-heat loading test in which the temperature was maintained at 1400 °C measured by a radiation thermometer with a continuous beam (Fig. 3[b]). After 67 min, the foil was broken at the beam spot. These results show that graphite has high endurance under high beam impact and high heat loading.

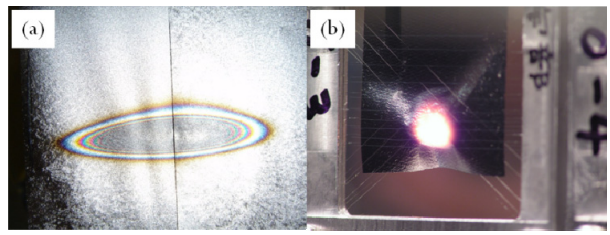

Figure 3: (a) After a long-run test, beam evidence was clearly visible at the beam spot as a color pattern resembling Newton's rings, indicating decreased thickness. (b) Heat loading test at 1400 °C.

TARGET FABRICATION

Alumina Frame

Alumina frames (Al_2O_3: 99.6%, made by Ariake Materials Company Ltd.) of three sizes were used for the 3-50 BT's targets: 200^H × 200^V, 250^H × 250^V, and 310^H × 190^V mm^2. All were 3 mm thick, and the unflatness was made to be less than 100 μm because of the small focal depth of the laser beam used for foil cutting, as described below. On its surface, electrodes for contact with the ribbon and a wiring pattern for signal readout were printed using AgPt material by thick-film technology (Minotos Engineering). The material adheres strongly to alumina. Au material was also used to connect the electrodes to read-out connectors on the cabling.

Electro-conducive Binder

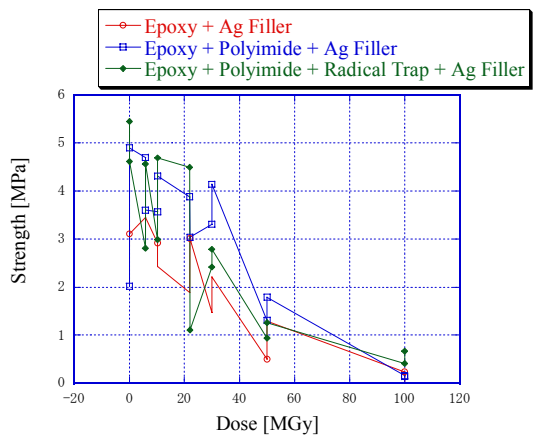

Figure 4: Pulling strength test on attached sample using three types of electro-conductive binder after irradiation. No major difference was found between them.

An electro-conductive binder developed by CITIZEN ELECTRONICS Co., Ltd. was used to attach the foil to the printed electrode on the frame. The binder has heightened radiation resistance because it combines

polyimide with its main component of halogen-free epoxy with hybrid silver grains; moreover, it includes a radical trap component. An irradiation test with gamma rays from ^{60}Co at up to 100 MGy in total dose was conducted. After 50 MGy of exposure, the pulling strength remained about 1 MPa, as shown in Fig. 4. In practice, this binder was used in the long-run beam test of foil endurance mentioned above, and it did not appear to cause problems. An outgassing rate from the attached surface of 1×10^{-9} Pa·m^3/s/cm^2 was obtained after 100 h of evacuation.

Ribbon Fabrication by Laser Cutting

For accurate beam measurement, every ribbon must have the same area. To achieve precise widths and positions of the graphite ribbons on the frame, a laser cutting method was adopted. First, graphite foil was applied to the electrodes by using the electro-conductive binder at an appropriate tension. The ray of an excimer laser was employed for cutting because of the relatively weak shock it imparted to the graphite. The spot size of the ray was about 30 μm, and its focal depth was +/-50 μm. Since the graphite was hard but fragile under laser power impact, cutting was done by using a power-attenuated ray and tracing the same line several times. The positional accuracy of the laser spot was about 10 μm. The cut ribbons and the final target are shown in Fig. 5(a) and (b), respectively.

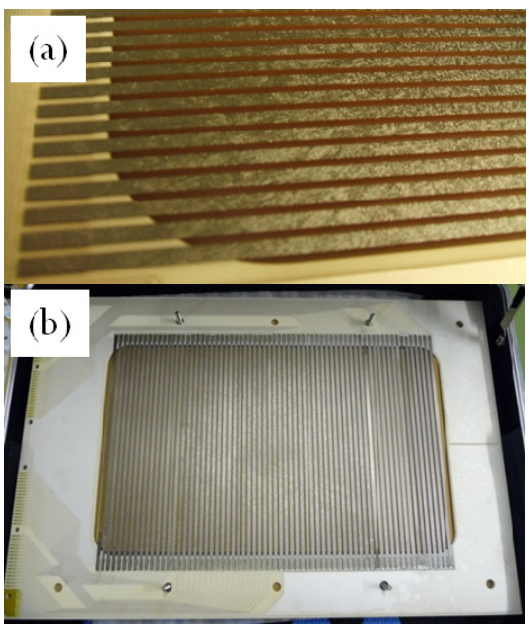

Figure 5: (a) Ribbon cut into 1 mm width as target for the slow-extraction beam line. (b) Largest target for injection point of the MR; frame inside area is $310^{H} \times 190^{V}$ mm^2. Ribbon is 3 mm wide and is used in a 67-channel array.

ELECTRON-EMISSION UNIFORMITY

The electron emission rate should be uniform at every point on the surface of the ribbon for accurate measurement. To investigate the emission uniformity, a beam test was conducted at the National Institute of Radiological Science (NIRS) with a C^{6+} beam whose energy was 6 MeV/n. In the test, a small target with a size of 50 × 50 mm^2 was used; ribbons were arrayed on it with a 2 mm pitch and 1 mm width. Each ribbon consisted of a different foil (Fig. 6[a]). The frame was swept in the direction perpendicular to the beam to measure the beam profile using each ribbon. Assuming a stable beam, the profile cannot change during target sweeping. Fig. 6(b) shows examples of the results for three different types of graphite. One was fired at 3000 °C; the other two are from two different parts of a graphite sample fired at 2600 °C. The measured profiles were suitably fit by a Gaussian. When they were parameterized with a standard deviation of σ, the fitting differences of each curve are within 0.02%. Finally, graphite fired at 2600 °C was used in actual target. Several beam tests with different graphite samples were conducted as described above during the development period, and the difference in emission rate was confirmed to be sufficiently-less than 1%.

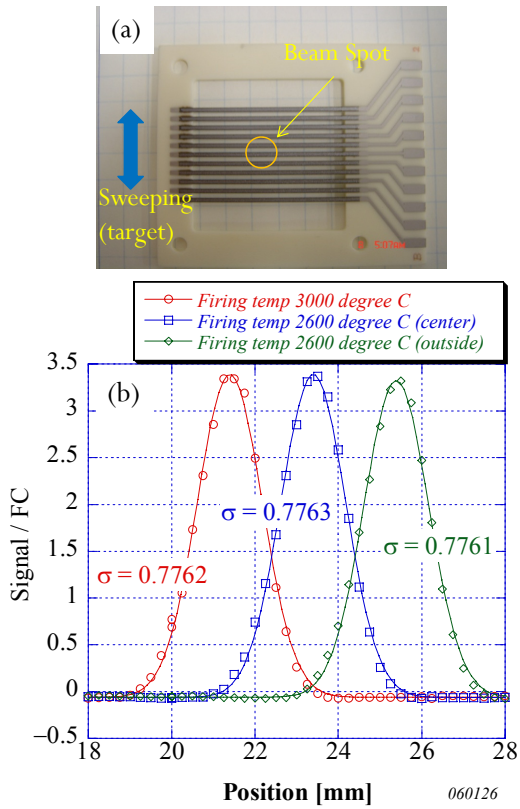

Figure 6:(a) Test target for emission-rate uniformity, (b) Sample test results.

EQUIPMENT AND MEASUREMENT SYSTEM

Equipment

A photograph of the standard multi-ribbon profile monitor (MRPM) equipment is shown in Fig. 7. The motion system used a type of linear motion because shocks during target movement could be avoided, and cables situated inside the vacuum did not move at

anytime, avoiding cable trouble. The MRPMs installed around the MR are shown in Fig. 8. In the near future, four and two monitors are scheduled for installation on the 3-50 BT and the slow extraction line, respectively.

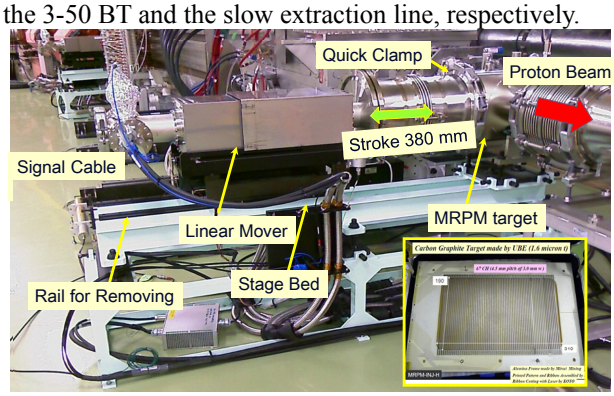

Figure 7: MRPM equipment at the MR injection point.

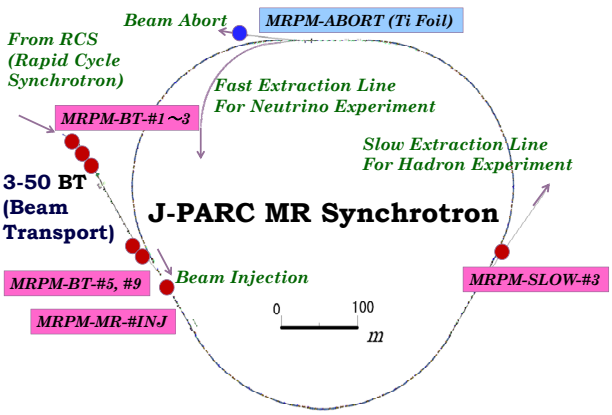

Figure 8: Installed MRPMs at beam transport line and MR. Titanium foil 10-μm thick was employed as a target for the beam abort line. Its ribbons were 50 mm wide and 750 mm long; they were arrayed with 15 channels for both horizontal and vertical targets situated in a beam pipe 850 mm in diameter.

Cable

Inside a vacuum, a vacuum-tight twisted pair cable covered with alumina fiber and glass fiber was used for charge signal transmission. Its outgassing rate was 4×10^{-8} Pa·m^3/s/m after 100 h of evacuation. In a standard MRPM, although this cable was 1.1 m long and consisted of 66 pairs, the actual vacuum pressure was on the order of 10^{-6} Pa. In air, a 34-channel 1.5D coaxial cable assembly developed by Fujikura Ltd. was used. Its shielding was triple layered type for weak charge-signal of 100 pC or less. It has three layered shields: two layers of an electromagnetic shield made of 0.6-mm-thick iron, and a corrugated electrostatic shield made of 0.7-mm-thick aluminum positioned inside of iron shields. The signal was transmitted via this cable assembly without amplification for a length of ~400 m from the equipment to the electronics situated at the MR local control room. In the cable assembly, each coaxial cable has a shield made of aluminized tape, and the cross talk was -60 dB or less in the frequency range of DC to 100 kHz.

Electronics

For signal processing, a module of 32-channel CAMAC-MWPM charge ADC (Fig. 9) was employed. It was in use at the KEK-NML beam line until 2004. For signal input, a cascaded amplifier and integration circuit (time constant 3–30 μs) in a hybrid package were used. Its gain was 400, and its input impedance was 1 kΩ. A background signal consisting of 33 channels of the outermost ribbon's signal was subtracted from each integrated signal. Finally, the signal was processed with analog-to-digital conversion with a bit depth of 10.

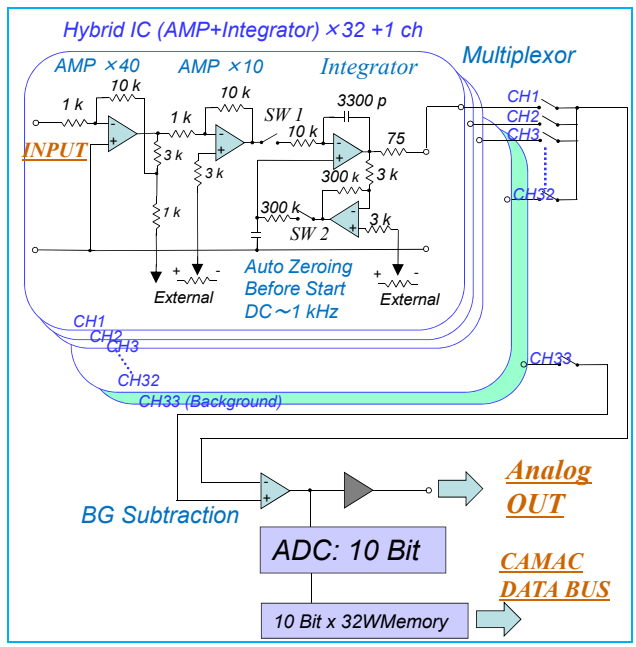

Figure 9: Circuit layout of 32-channel CAMAC module.

BEAM MEASUREMENT

High-intensity Beam

Beams with an intensity of 1×10^{13} ppb that have been injected to the MR for obtaining beam power of 100 kW were successfully measured.

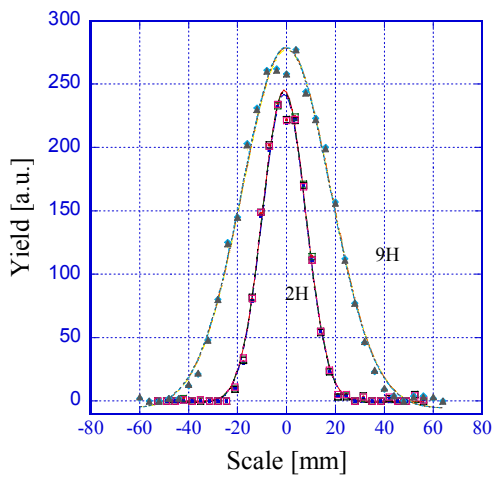

Figure 10: Profiles of beam intensity of 1×10^{13} ppb.

Figure 10 shows a plot of the horizontal output of two monitors, #2H and #9H, which were placed at upper stream and its end, respectively, in the 3-50 BT. Both were superimposed using data from five arbitrarily selected other times and were fitted by a Gaussian. The results show that the deviations were sufficiently small, and both the measurements and the transported beams have good reproducibility. During these measurements, signals were attenuated by 1/2000.

Plateau

Plateau curves with various voltages applied to the electron-collection electrodes were measured for beams having intensities of 1×10^{13} and 4×10^{11} ppb with an electrometer (Keithley 6517A).

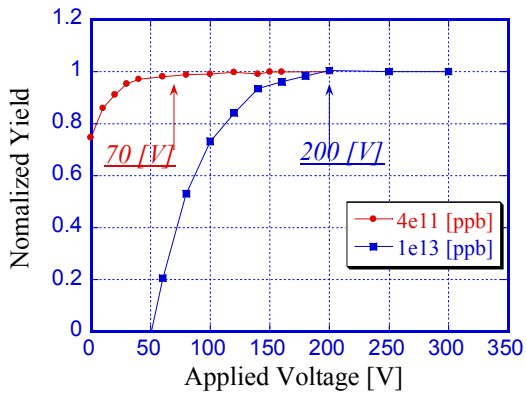

Figure 11: Plateau curves.

Figure 11 shows the normalized curves. The starting plateau voltages were about 200 V and 70 V, respectively. In particular, in the former case, when the applied voltage was 50 V, the emission yield was zero. The electric potential near the ribbon surfaces is believed to be reduced to less than zero by the space charge effect because of the high beam density of secondary electrons. During measurement, the three-sigma beam sizes were $35^{H} \times 16^{V}$ mm^2 and $80^{H} \times 30^{V}$ mm^2, respectively, and the bunch lengths of each were about 100 ns.

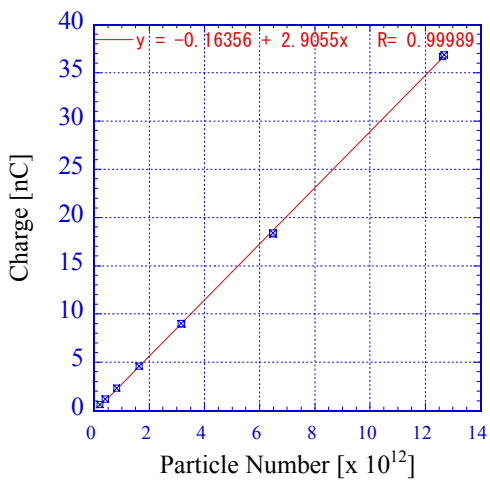

Figure 12: Linearity curve.

Linearity

The linearity was measured with the electrometer (Fig. 12) when a voltage of 250 V was applied to one electron-collection electrode. The beam bunch intensity ranged between 2×10^{11} and 1.2×10^{13} ppb. The linearity was good, and the applied voltage was sufficient to overcome the space charge effect. The slope of the line indicates the electron emissivity from both surfaces of the graphite. Linear fitting yielded a result of 2.9055×10^{-12} nC/proton at 3 GeV, which can be converted to a value of 0.018 electrons/proton.

CONCLUSION

For a high-intensity beam such as J-PARC's, a secondary-electron-emission type beam-profile monitor using graphite ribbons was developed. The length of the ribbons was more than 200 mm, and the non-uniformity of the rate of electron emission from its surface was sufficiently-less than 1 %. It detected high-intensity beams of up to 1×10^{13} ppb at a beam energy of 3 GeV with good linearity of electron-emission yield. Since the graphite in the ribbons is as thin as 1.6–2 μm, the beam energy loss and energy deposition decreased to 0.8 keV/foil and 5.1×10^{-3} J/bunch/foil, respectively, at a beam energy of 3 GeV and intensity of 4×10^{13} ppb, which are the design values.

ACKNOWLEDGMENT

This development was supported by a research project with heavy ions at HIMAC by NIRS; we thank the entire crew of HIMAC for their kind support. The authors also thank Dr. I. Sugai and Dr. Y. Takeda (KEK) for their steady work on high-temperature beam-endurance tests of the graphite foil; to Dr. Y. Akao (CITIZEN ELECTRONICS Co., Ltd.) for developing an excellent electro-conductive binder; to Mr. T. Iwanaga (Ariake Material Co., Ltd.) for fabricating large alumina frame with fine flatness; and to Mr. S. Nakazawa and Mr. Y. Matsumoto (Koyo Seiko Co., Ltd.) for conducting inimitable laser cutting of the graphite.

REFERENCES

[1] A. Miura, et al., "Operational Performance of Wire Scanner Monitor in J-PARC LINAC", IPAC'10, Kyoto, Japan, May 2010, p. 1008.
[2] S. Meigo, et al., "A Study of Proton Beam Profile on the Target at JSNS", Proc. of 19th Meeting on Collaboration of Advanced Neutron Sources, Grindelwald, Switzerland, March 2010.
[3] S. Hiroki, et al., "Multi-Wire Profile Monitor for J-PARC 3 GeV RCS", EPAC08, Genoa, Italy, June 2008, p.1131-1133.
[4] S. E. Kopp, et al., "Beam Test of A Segmented Foil SEM Grid", NIMA554(2005)138-146.